ARMY RESEARCH LABORATORY

A Survey of Compression Studies on Silicon Carbide (SiC)

by Dattatraya P. Dandekar

ARL-TR-2695 March 2002

The findings in this report are not to be construed as an official Department of the Army position unless so designated by other authorized documents.

Citation of manufacturer's or trade names does not constitute an official endorsement or approval of the use thereof.

Destroy this report when it is no longer needed. Do not return it to the originator.

Army Research Laboratory
Aberdeen Proving Ground, MD 21005-5066

ARL-TR-2695 **March 2002**

A Survey of Compression Studies on Silicon Carbide (SiC)

Dattatraya P. Dandekar
Weapons and Materials Research Directorate, ARL

Abstract

Compression of a solid material under plane shock wave propagation/ loading can provide information related to change in density and shear strength with pressure/stress of the material under inertial confinement. The present work surveys and analyzes the existing shock compression and high-pressure data on silicon carbide to provide pertinent information to material modelers and others for use in their work related to this material. It also points out a set of investigations that needs to be carried out to complement the existing data.

Acknowledgments

The author appreciates the support of Dr. D. W. Templeton, U.S. Army Tank-Automotive Research, Development, and Engineering Center, Warren, MI, for making this report possible.

INTENTIONALLY LEFT BLANK.

Contents

INTENTIONALLY LEFT BLANK.

List of Figures

INTENTIONALLY LEFT BLANK.

List of Tables

INTENTIONALLY LEFT BLANK.

1. Introduction

Silicon carbide (SiC) is a material of considerable interest because of its technological applications as superabrasive, high-temperature electronic material, as well as blue light emitting diode, and it is a material component of an armor system [1–3]. All SiC structures are made up of a pair of hexagonal layers, one made up of carbon atoms and the other of silicon atoms. The two simplest systems for SiC are cubic zincblende (β-SiC) and wurtzite structure (α-SiC). Both have densities of 3.21 Mg/m^3. β-SiC transforms to α-SiC above 1873 K. SiC is also reported to exist in over 100 polytypes under the ambient condition [4]. The different polytypes are generated by the stacking sequence of a number (N) of SiC pair layers in the cubic [111] direction within a unit cell of the cubic (C), hexagonal (H), or rhombohedral (R) structure. Numbers are attached to each polytype according to the number of pair layers within the stack. These polytypes differ with respect to temperature at generation [5]. 2H-SiC and 3C-SiC are formed at 1773 and 1873 K, respectively. 4H-SiC, 6H-SiC, and others are formed at and above 2273 K. 6H is the most stable of these polytypes at temperatures between 2473 and 2873 K. Polytypes 2H, 3C, 4H, 6H, and 15R occur most frequently. As yet, a complete set of values of all the elastic constants of either form of SiC is not available.

Several investigations deal with the hydrostatic compression [6–9] of SiCs. In addition, over the past four decades a large number of shock wave compression experiments have been conducted on polycrystalline SiCs to determine their compressibility and shear strength retained under plane shock wave compression [10–20]. This list excludes shock wave investigation studies dealing with spallation in SiC because Dandekar and Bartkowski [21] recently covered this subject. The type of SiC used in earlier shock compression investigations was not always unambiguously identified except in terms of densities and in some cases chemical compositions. But, if a description of processes employed to produce SiC was provided and then based on the stability of the various polytypes, one may infer structure and polytype from such a description. In recent years, the type of SiC used in experiments is generally identified, explicitly making comparisons of the results obtained by the various investigators easier and more meaningful. Such explicit identification also provides a margin of error in the values of the various parameters like compressibility of the material and shear strength retained by a specific type of SiC under plane shock wave propagation. This work summarizes the results of the existing hydrostatic compression data and shock wave compression data on silicon carbide in the open literature.

2. Compression of SiC

2.1 Hydrostatic Compression

The results of hydrostatic compressions of 3C-SiC, 6H-SiC, and 15R-SiC, determined by high-pressure x-ray diffraction experiments, are reported by Strossner et al. [6], Aleksandrov et al. [7], Bassett et al. [8], and Yoshida et al. [9]. These investigators used diamond-anvil cells to generate high pressure in SiCs. The pressure attained in the material was estimated from the calibration data of Mao et al. [22], or from volumetric compression of gold using the equation of state of Heinz and Jeanloz [23]. Whereas Aleksandrov et al. [7] confined SiC in a compressed helium medium that produced a hydrostatic pressure environment estimated to be over 30 GPa, Bassett et al. [8], Strossner et al. [6] and Yoshida et al. [9] confined their materials in a mixture of sodium chloride and gold, and methanol, ethanol, and water, respectively, to produce a hydrostatic pressure environment in their samples. The results of these investigations on crystalline SiC are summarized in Table 1.

Table 1. Bulk modulus (B_0), pressure derivative of the bulk modulus (B'_0), and maximum pressure (P_{max}) to which experiments were carried out in SiC in various static pressure investigations.

Type	B_0 (GPa)	B'_0	P_{max} (GPa)	Reference
3C	248 ± 9	4.0 ± 0.3	25	[6]
3C	227 ± 3	4.1 ± 0.1	42	[7]
15R	224 ± 3	4.3 ± 0.1	45	[7]
6H	230 ± 4	4.0 (assumed)	68	[8]
3C	260 ± 9	2.9 ± 0.3	105	[9]
6H	260 ± 9	2.9 ± 0.3	95	[9]

It is of interest to deal with the status of elastic constant measurements in various SiC's. Lambrecht et al. [24] gave a complete and critical review of experimental measurements of elastic constants of SiC. There has been no direct determination of the full set of elastic constants for either 3C-SiC or hexagonal polytypes of SiC, as single crystals of 3C-SiC and 6H-SiC have been generally unavailable. Thus, estimates of elastic constants of a polycrystalline SiC must be made on some assumption. Hofmann et al. [25] used the bond-charge model in conjunction with the measured Raman spectra, infrared absorption, and reflectivity measurements and luminescence studies on 3C, 2H, 4H, 6H, 10H, 15R, and 21R SiC to obtain the elastic constants of various polytypes of SiC. They calculated the values of elastic constants obtained from the limited sound wave

velocity measurements, resonance experiments, and optical and phonon measurements. Their results indicate that the values of elastic constants of 3C, 2H, 4H, and 6H-SiC are fairly close to one another. The estimated values of bulk modulus of polycrystalline 3C-SiC range between 225 and 247 GPa [24]. The estimated value of the bulk modulus for polycrystalline 6H-SiC based on experimental values of single crystal elastic constants C_{11}, C_{33}, and C_{12} measured by Arlt and Schodder [26], and the estimated value of C_{13} by Hofmann et al. [25] is 273 GPa. It is difficult to calculate margin of errors in these calculated values of bulk moduli for these two polytypes of SiC. The measured value of the bulk modulus of polycrystalline SiC-B, which is primarily 6H-SiC, from the ultrasonic measurements reported by Dandekar and Bartkowski [21] is 221 ± 2 GPa (Table 2). This table also gives the properties of two other types of polycrystalline SiC. Holmquist et al. [27] provide these properties for other SiCs. The accuracies of sound velocities and scatter in the sound wave velocities between samples of KT-SiC were each reported to be within 2% [12]. The properties of SiC-B and SiC-N given in here were reported by Dandekar and Bartkowski [21].

Table 2. Properties of various polycrystalline SiCs.

Property	KT SiC [12]	SiC-B [21]	SiC-N [21]
Grain Size (μm)	–	2–10	1–8
Density (Mg/m^3)	3.09	3.215 ± 0.002	3.227 ± 0.001
Pore Volume Fraction	0.04	0.002	–
Elastic Wave Velocity (km/s)	–	–	–
Longitudinal	11.4	12.198 ± 0.026	12.262 ± 0.001
Shear	7.27	7.747 ± 0.018	7.77 4± 0.005
Bulk	7.71	8.29 ± 0.03	8.354 ± 0.006
Elastic Modulus (GPa)	–	–	–
Young's	378	448.4 ± 2.1	454.0 ± 0.6
Shear	163	193.0 ± 0.9	195.0 ± 0.2
Bulk	184	221.1 ± 1.8	225.2 ± 0.3
Poisson's Ratio	0.157	0.162 ± 0.003	0.164 ± 0.001

The values of B_0 for both 3C and 6H SiC differ significantly from each other in these hydrostatic compression investigations (Table 1). The reasons are difficult to single out with any confidence. Most likely, the differing pressure medium used in these investigations leads to a departure from differing amounts of hydrostaticity in these investigations at differing pressure levels. The calculation of pressure at a given compression can easily lead to the observed difference especially in hard, brittle, and incompressible material like SiC. For example, Aleksandrov et al. [7] found that the magnitude of pressure at a given compression for 3C-SiC calculated from their own calibration and by adopting the one suggested by Mao et al. [22] differ by as much as 4 GPa at

14% compression. The values of pressure at this compression are 40 and 44 GPa, resulting in a 10% variance with calibration method. This also implies that the estimates of B'_0 from these types of experiments may be subject to an even larger variability. Further, because Segletes [28] showed that

$$\Gamma_{Slater} = -1/6 + 0.5\, B'_0, \tag{1}$$

the variation in B'_0 is on scale of Γ variations, which are quite large and can be the source of even larger variability.

The compression curve obtained for SiC from these studies may be presented either in the form of the Birch-Murnagham finite strain equation of state, as is customary and favored by the investigators in the field of static high pressure, or the equation of state based on the linear shock velocity (U_s) and particle velocity (u_p) relationship observed in solids in the field of shock wave compression.

Birch [29] showed that the isentropic compression using the Eulerian definition of finite strain, i.e.,

$$f = [(V_0/V)^{2/3} - 1]/2, \tag{2}$$

is given by

$$P = 3\, B_0 f(2f+1)^{2.5} [1 + a_1 f + a_2 f^2 + ...], \tag{3}$$

where V is reciprocal of density, a's are constants, and P is the pressure. The subscript 0 indicates the initial/ambient specific volume.

The equation of state based on the linear relationship between shock velocity (U_s) and particle velocity (u_p), given by

$$U_s = C_0 + s\, u_p \tag{4}$$

yields

$$P_H = \rho_0 (C_0)^2 \eta/(1 - s\,\eta)^2, \tag{5}$$

where $\eta = 1 - (V/V_0)$ and P_H is the Hugoniot pressure.

Under the Birch-Murnaghan assumption, $a_2 = 0$, Jeanloz and Grover [30] showed that

$$a_1 = 1.5(B'_0 - 4) = (6s - 7.5) \tag{6}$$

and

$$a_2 = 215/6 - 60s - 3\,\gamma_0 s + 27\, s^2. \tag{7}$$

In equation (7), γ_0 is the Gruneisen parameter at the ambient condition. Further Jeanloz and Grover [30] showed that equations (4) and (6) are identical for a material if the values of γ_0 and B'_0 lie between the range of 0.8–2.6 and 4–6, respectively. It should be noted that if terms involving a_2 are neglected and the

value of B'_0 determined from the static high-pressure experiment is 4, then equations (4) and (6) will give identical results if and only if the value of s from shock wave experiments is determined to be 1.25. In case this is not true, the compression curves obtained from the static and shock measurements will differ from one another. The significance of this difference at a given compression of a material is application dependent. For example, the magnitude of pressures for 3C and 6H SiC at 23% compression obtained from these two equations for the experimental results reported by Yoshida et al. [9] are 98 and 101 GPa, respectively.

Figure 1 shows the mean volumetric compression of 6H-SiC obtained by Bassett et al. [8] and Yoshida et al. [9]. The experimental data coordinates are not shown in this figure to preserve the clarity. This figure also shows the lower and the upper limits of the volumetric compression of 6H-SiC based on the results of Yoshida et al. [9]. The lower and the upper limits of the compression are obtained using the values of B_0 and B'_0 as 251 GPa and 2.6, and 269 GPa and 3.2, respectively (Table 1). This figure shows that the compressions of 6H-SiC determined in these two investigations are very close to one another even though the values of bulk modulus and its pressure derivatives determined in these two investigations are beyond the range of experimental uncertainties reported by these investigators. Bassett et al. [8] assumed the value of the pressure derivative of the bulk modulus to be 4.

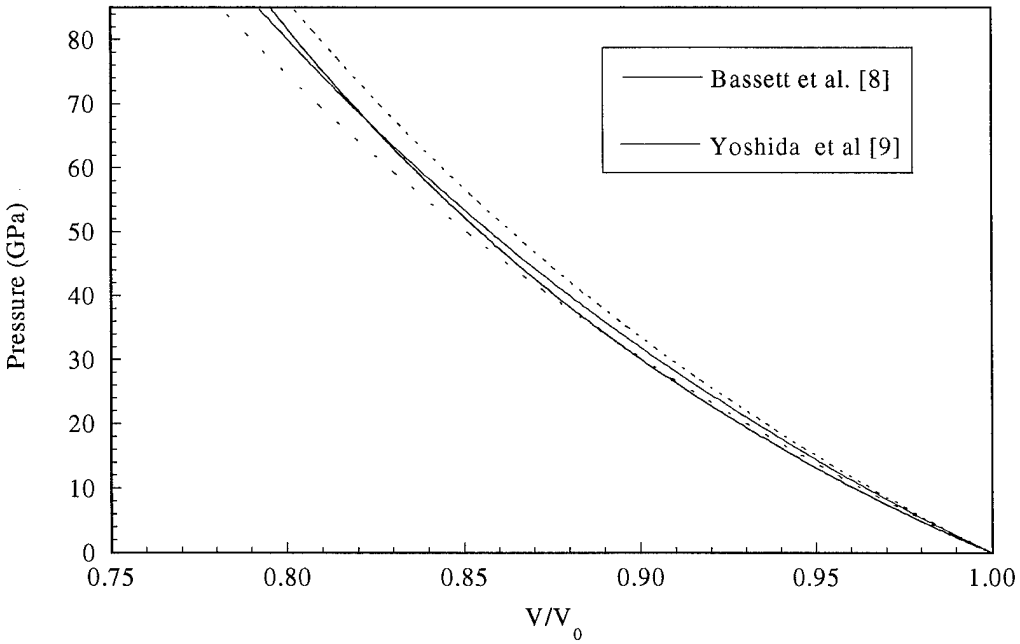

Figure 1. Compression of 6H-SiC from static high-pressure x-ray diffraction data.

Finally, Yoshida et al. [9] found that 3C-SiC undergoes a phase transition to a rock salt type structure at and above 100 GPa, with an accompanying volume reduction of 20.3%. This phase transition is reversible and goes back to the original 3C phase when the pressure is lowered to 35 GPa. Thus, the persistence of the rock-salt phase down to 35 GPa from 100 GPa amounts to a large hysteresis accompanying the phase transition. They did not observe any indication of phase transition in 6H-SiC to 95 GPa.

Liu and Vohra [31] reported the results of Raman study in 6H-SiC to 95 GPa in a diamond cell anvil. Based on the Raman spectra of 6H-SiC, they concluded that the 6H-SiC structure is stable to 95 GPa. Their sample became optically transparent at this pressure. But the relative softening of the Gruneisen parameter for the longitudinal optical (LO) mode compared to the transverse optical (TO) mode at elevated pressure suggested to them that it might be a precursor to a phase transition in the range of 100–200 GPa. Further, their observation of initial increase in transverse effective charge to 40 GPa and an observed decline upon further increase in pressure suggested that 6H-SiC is more ionic when compressed to 40 GPa, but becomes more covalent upon further increase in the pressure. Whether this leads 6H-SiC to become more incompressible and/or retain lower or higher shear stresses at shock-induced stress above 40 GPa remains to be ascertained through future investigations.

2.2 Hydrodynamic Compression

Shock compression of a material is affected by the magnitude of porosity and impurities present in it, which is not the case for in-situ high-pressure x-ray diffraction measurements discussed previously. McQueen et al. [10] and Marsh [11] published shock compression data on SiC, with density varying between 2.33 and 3.12 Mg/m^3. Gust et al. [12] measured shock compression of SiC with a density of 3.09 Mg/m^3. The material used by Gust et al. [12] was hot-pressed and manufactured and marketed by Carborundum Company under the name Type KT SiC. They reported the impurities in KT SiC. The material was α-SiC, but no identification about the polytype was provided. Based on the similarity of the highest density of SiC used by McQueen et al. [10], it is presumed that their material was also obtained from the Carborundum Company. Sekine and Kobayashi [13, 14] recently measured shock compressions of 6H-SiC and 3C-SiC to 160 and 150 GPa, respectively. 6H-SiC material used was manufactured by Cercom Inc. and is marketed as SiC-B. Sekine and Kobayashi did not mention the source of 3C-SiC, and only two experiments were performed. The results of two experiments on 3C-SiC were reported to be consistent with those of Yoshida et al. [9]. The Hugoniot Elastic Limit (HEL) of 3C-SiC was determined to be 12 GPa. Grady [15] attempted to measure the hydrodynamic compressibility of SiC through shock compression of mixture samples of α-silicon carbide powder and copper. The shock compression data reported by

Sekine and Kobayashi [13, 14] complements the results of low magnitude shock compression experiments designed to measure stress wave profiles and obtain the associated properties of SiC-B and other α-SiC, such as the HEL, and the nature of inelastic deformation, shear strength retained under plane shock wave compression, and release behavior reported in references [16–20].

Hydrodynamic compressions of these materials represented by the bulk modulus and pressure derivative of the bulk modulus are summarized in Table 3. Figure 2 shows a plot of shock compression data generated by these investigators as pressure vs. specific volume. In this figure, the data points denoted by HEL are at or below the HEL; PL1 indicate inelastic deformation of SiC, and PL2 indicate the transformed phase of SiC. This figure shows that the compression data of McQueen et al. [10], Marsh [11], and Gust et al. [12] are consistent with each other. The shock compression data of almost fully dense 6H-SiC reported by Sekine and Kobayashi [13, 14] is stiffer than of the low-density KT SiC. The data obtained by Sekine and Kobayashi labeled PL2 roughly follows the initial trajectory of the McQueen et al. [10] data above 100 GPa. The curve in this figure represents the compression of 6H-SiC obtained by using the values of bulk modulus and its pressure derivative given in Table 3 and relation (5).

Table 3. Density (ρ_0), HEL, B_0, and B'_0 for SiCs used in shock compression investigations.

Type	ρ_0 (Mg/m^3)	HEL (GPa)	B_0 (GPa)	B'_0	P_{max} (GPa)	Reference
KT-SiC	3.12	8 ± 3	184–201	2.8–3.4	110	[10, 11]
6H-SiC	3.22	18.0 ± 0.7	230[a]	4.6	105	[13, 14]

[a] Sekine and Kobayashi [13, 14] took the value of B_0 from Bassett et al. [8] for their analyses.

Gust et al. [12], based on their own data and the data reported by McQueen et al. [10], suggested the existence of two phase transitions in their SiC. The first transition in SiC was estimated to occur at 24 GPa and the second one at around 96 GPa. Sekine and Kobayashi [13] detected only one phase transition in 6H-SiC at 105 ± 4 GPa accompanied with a volume reduction of 15 ± 3%. The transition was not complete until a pressure of 137 ± 4 GPa was reached. The structure of the new phase of the material is suggested to be rock salt structure. Further details about this transition may be found in reference [13].

2.3 Comparison of Hydrostatic and Hydrodynamic Compression of 6H-SiC

The density of this type of SiC is 3.215 (Mg/m^3). The value of the bulk modulus (B_0) at the ambient condition obtained from ultrasonic wave velocity measurements is 221 GPa (Table 2). The bulk modulus obtained from ultrasonic wave velocity measurements is the adiabatic modulus. The values of B_0 reported from in-situ x-ray diffraction measurements at static high pressure are the

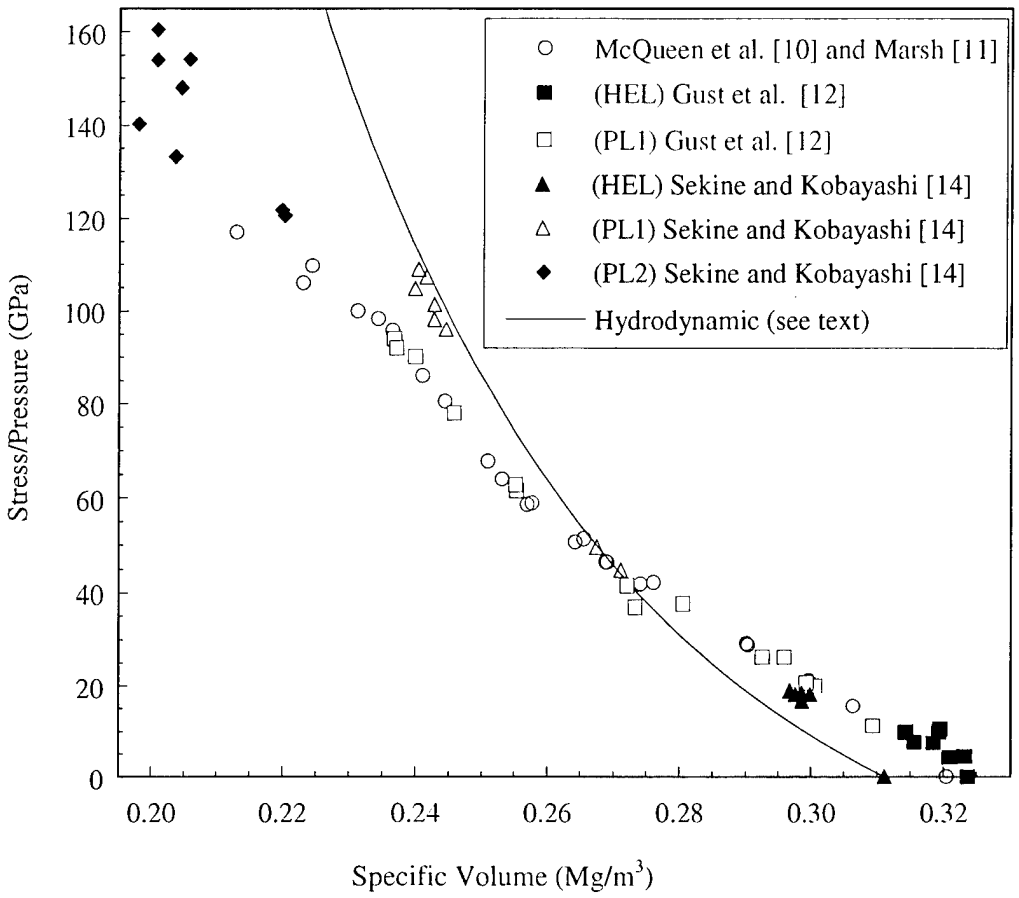

Figure 2. Shock compressions of SiCs.

isothermal bulk moduli and range from 230 to 260 GPa (Table 1). The ratio of the adiabatic and isothermal bulk modulus of SiC, based on its value of Gruneisen parameter (1.2) and volumetric thermal expansion coefficient 13.8 × 10-6 K-1 is 1.005. Thus, the difference between the magnitude of bulk modulus obtained from ultrasonic wave velocities and x-ray diffraction measurements is insignificant. No measurement of bulk modulus is available from the shock wave compression data. Sekine and Kobayashi [13] assumed a value of 230 GPa for the bulk modulus reported by Bassett et al. [8] and obtained a value of 4.6 for B'_0. The value of B'_0 obtained from their data by using 221 GPa as the value of bulk modulus determined from the ultrasonic velocity measurements is 4.8, not very different from the value of 4.6. However, a regression analysis of their data indicates that the uncertainty in the value of B'_0 is ±0.4. The value of B'_0 obtained from the hydrostatic compression measurements is 2.9 ± 0.3 (Table 1). It is of interest to note that the estimated values of B'_0, based on value of Gruneisen parameter as 1.2 and using Slater and Dugdale-McDonalds relations, are 2.7 and 3.4, respectively. Since ultrasonic wave velocity measurements provide the most accurate value of bulk modulus at the ambient condition and are more

likely to be representative of 6H-SiC used in large-scale applications rather than those obtained from the x-ray diffraction measurements at high pressures, it is preferable to use a value of 221 GPa for B_0 of 6H-SiC. The reason for this is that x-ray diffraction measurements at static high pressures provide the compression of SiC itself and are not influenced by porosity or free impurities in the sample. A larger scatter in the value of B_0 of 6H-SiC reported in Table 1 may arise from a host of sources, including the one related to the differentiation of the pressure volume data. Under an ideal condition, one would expect the value of the bulk modulus for a material obtained from high-pressure x-ray diffraction measurements to be consistent with the ultrasonic value and also more consistent with one another than reported for 6H-SiC by Bassett et al. [8] and Yoshida et al. [9].

The compression curves of 6H-SiC obtained by using 221 GPa for the value of B_0 and 2.9 ± 0.3 and 4.6 for the values B'_0 are compared with the compression curve generated from the results of compression and shear wave velocity measurements to characterize the shocked state of 6H-SiC by Yuan et al. [20]. Figure 3 shows the results such calculations. This figure shows that the compression curves of 6H-SiC obtained by Yuan et al. [20] and Sekine and Kobayashi [13] are almost identical to one another to 60 GPa. It suggests that one may use the equation of state generated from the data of either of these two investigations with some confidence to at least 90 GPa. Numerical simulations are generally done by expressing pressure as a function of the third degree polynomial of μ, where μ is defined as $\{(V_0/V)-1)\}$. Such a truncated equation of state for 6H-SiC using the data from Sekine and Kobayashi [13] may be given by

$$P = 221\,\mu + 398\,\mu^2 + 283\,\mu^3. \qquad (8)$$

Figure 4 shows that relation (8) actually represents the compression of 6H-SiC very well to 60 GPa and satisfactorily to 90 GPa. This suggests that relation (7) can be used to calculate compression of an intact 6H-SiC to at least 90 GPa.

2.4 Shear Strength of 6H-SiC

Shear strength of SiC-B under shock compression through simultaneous measurements of longitudinal and lateral stress measuring has been measured by Feng et al. [19] and Bourne et al. [18]. It is of interest to calculate the values of shear stress sustained by 6H-SiC obtained from the equation of state given by relation (8) and the longitudinal stress measured near and above its HEL in references [16, 18, 19] and compare them with the values obtained from the measurements of lateral and longitudinal stress under shock loading. The values of longitudinal stress and the associated volume change needed for calculations were given only in the paper published by Feng et al. [19]. The relation between the longitudinal stress (σ_L), pressure (P), and shear stress (τ) at a given strain is given by

$$\tau = 0.75\,\{\sigma_L - P\}. \qquad (9)$$

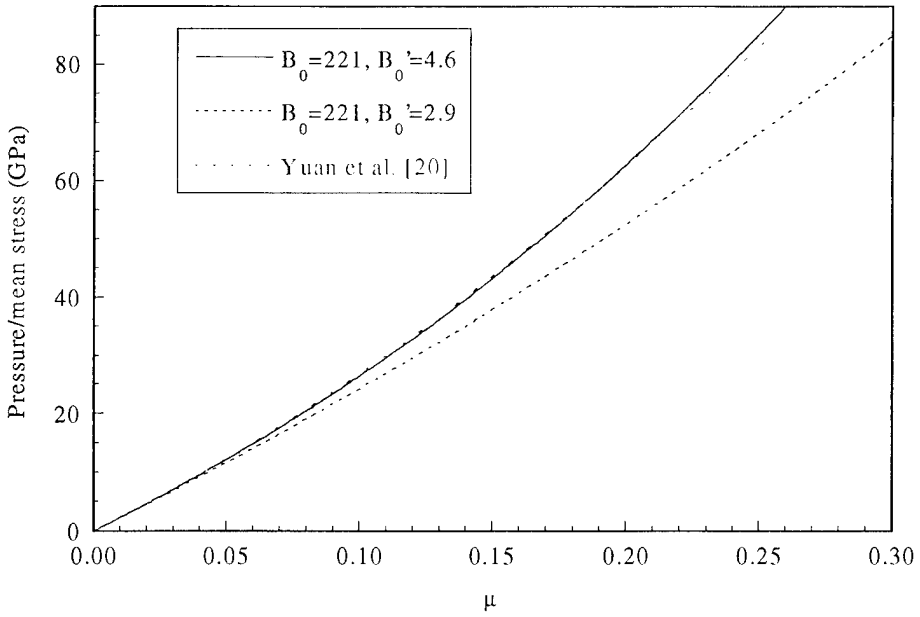

Figure 3. Hydrodynamic compression of 6H-SiC.

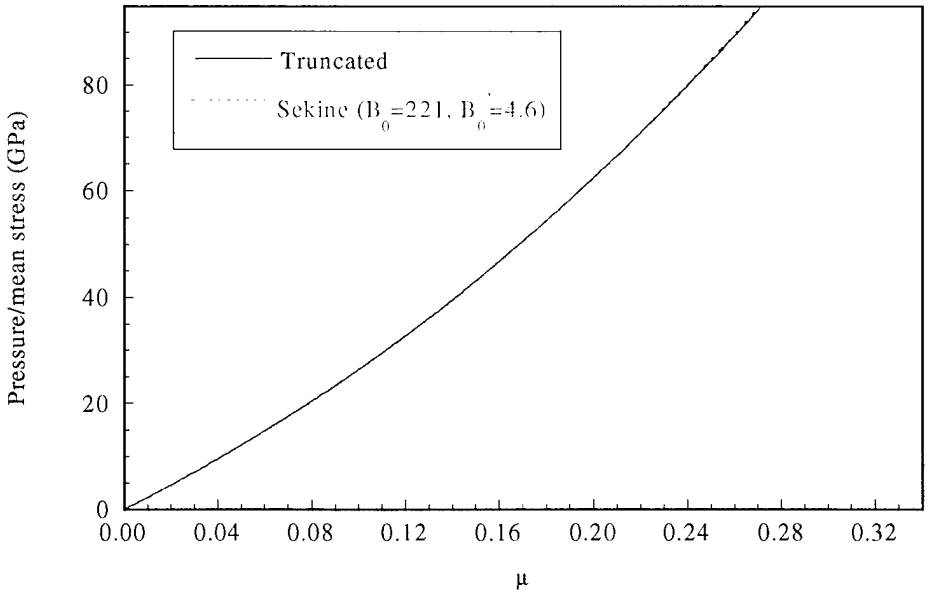

Figure 4. Comparison of compressions of 6H-SiC generated from relations (5) and (8).

Table 4 gives the results of the calculations. This table shows that the calculated values of shear stress and those obtained through the simultaneous measurements of longitudinal and lateral stresses agree with one another. The highest magnitude of longitudinal shock experiments were done by Crawford and reported by Feng et al. [17]. Results of two experiments reported in their Table 3 are given in Table 4 in this report. The values associated with (a) and (b)

Table 4. Measured and calculated values of shear stress sustained by 6H-SiC under plane shock wave compression.

Experiment No.	Stress (GPa)			μ	Calculated (GPa)	
	Longitudinal	Lateral	Shear		Pressure	Shear
Feng et al. [19]						
1	10.20	1.84	4.18	0.0209	4.80	4.05
2	12.90	2.34	5.28	0.0264	6.12	5.09
3	15.00	3.40	5.80	0.0312	7.29	5.78
4	16.00	3.60	6.20	0.0336	7.89	6.09
5	18.80	5.10	6.85	0.0412	9.80	6.75
6	20.90	6.94	6.98	0.0479	11.53	7.03
7	24.20	10.40	6.90	0.0610	15.03	6.88
Crawford's experiments reported by Feng et al. [17]						
SC-3 (a)	26.8			0.0875	22.8 ± 0.5	3.0 ± 0.4
SC-4 (a)	39.6			0.1314	36.9 ± 1.1	2.0 ± 0.8
SC-3 (b)	28.5			0.0785	20.2 ± 0.4	6.2 ± 0.3
SC-4 (b)	40.8			0.1237	34.4 ± 1.0	4.8 ± 0.8
Grady and Kipp [16]						
CE-4	27.6			0.075	19.2 ± 0.4	6.3 ± 0.3
CE-5	36.3			0.1087	29.4 ± 0.8	5.2 ± 0.6
CE-31	48.8			0.1534	45.0 ± 1.5	2.8 ± 1.1
Bourne et al. [18]						
1	16.7	3.3	6.7			
2	21.2	4.1	8.6			
3	23.4	6.7	8.4			

for these experiments are based on the calculation of longitudinal stress and μ using the elastic perfectly plastic model and the pressure-dependent strength, stress relaxation model proposed by Feng et al. [17]. These calculations indicate that the values of shear stresses based on the pressure-dependent strength, stress relaxation model are consistent with the other values of the shear stress given in this table.

Since the experimental results of Grady and Kipp [16] on α-SiC manufactured by Eagle–Picher was shown to coincide with the longitudinal shock of SiC-B in reference [17], the values of shear stress sustained by this material are also calculated and given in Table 4. The calculation shows a gradual reduction in the shear strength of the α-SiC with an increase in the longitudinal stress. Could this be related to the observed trend in the change in ionicity of the bonds in SiC and the development of covalency in SiC at around 40 GPa by Liu and Vohra [31]? The measurements by Bourne et al. [18] appear to be consistent with the measurements of Feng et al. [19], but tend to be a bit larger than their values at

longitudinal stress exceeding 21 GPa. There is clearly a need for such measurements at and above 20 GPa in SiC-B.

3. Concluding Remarks and Future Work

The findings of this report may be summarized as follows.

- The equation of state obtained from in-situ, high-pressure, x-ray diffraction measurements provides very precise values of compression (i.e., strain). The somewhat less precise measurement of pressure may be due to nonhydrostaticity of the pressure under which such measurements are made. A very good example are the measurements of compression obtained by Bassett et al. [8] and Yoshida et al. [9]. It was shown that while the compression loci for 6H-SiC obtained in these investigations were almost identical, the values of bulk modulus and its pressure derivative were not the same (Figure 1 and Table 1). Lack of knowledge about the complete set of elastic constants for a single crystal of 6H-SiC prevents making any judgment about the quality of measurements.
- The equation of state obtained from the shock compression measurements depends on the porosity and free impurities in materials indicated by the measurements on KT-SiC and 6H-SiC (Table 3). In the case of 6H-SiC, the investigations by Sekine and Kobayashi [13] and Yuan et al. [20] showed that the compression measured and expressed as a function of pressure and mean stress, respectively, are identical, and the value of bulk modulus used in both investigations was of a magnitude similar to that obtained from ultrasonic wave velocity measurements (Table 2 and Figure 3).
- The compression curves obtained from in-situ, high-pressure x-ray diffraction measurements of Bassett et al. [8] and Sekine and Kobayashi [13] are consistent with one another, but also owe their consistency to serendipity in the sense that these investigators obtained the value of only one of the two parameters (i.e., B_0 and B'_0, and made correct assumptions for the value of the remaining one).
- The experiments of Sekine and Kobayashi [13] yield a value of B'_0 4.6 ± 0.4.
- The third degree polynomial equation for use in numerical simulations for 6H-SiC (i.e., SiC-B) is given by

$$P = 221\,\mu + 398\,\mu^2 + 283\,\mu^3. \qquad (10)$$

- The procedure used to estimate shear stress/strength (τ) sustained by SiC-B from hydrodynamic compression and longitudinal stress measurements agree with the values obtained from the measured longitudinal and lateral

stress measurements (Table 4). To this date, the procedure has always yielded correct results for other materials [32, 33]. The value of τ appears to be constant, even though the collective trend indicates that SiC-B may be losing its shear strength with an increase in longitudinal stress beyond 40 GPa.

- There is a need to supplement the existing measurements of shear strength of SiC-B to validate the gradual reduction of shear strength at shock stresses beyond 24 GPa.
- There is no experimental data on any type of SiC to provide information pertaining to the effect of shock-induced damage on its subsequent dynamic response. Shock-reshock experiments on SiC, specifically SiC-B, will complement the existing data [34, 35].
- The extensive information available about the spall behavior of SiC-N needs to be supplemented by investigating shock compression and release response of SiC-N above its HEL.
- Finally, nonconvergence of the shock compression data for KT-SiC and 6H-SiC in Figure 2 suggests that it may be worth examining and analyzing the shock compression data of McQueen et al. [10] and Marsh [11] on α-SiC of densities 2.9, 3.0, and 3.1 Mg/m^3 to look into the feasibility of using their data to obtain compression response of damaged SiC. The assumption is that the different densities of SiC represent differing amounts of damage in the material.

INTENTIONALLY LEFT BLANK.

4. References

1. Olega, D., M. Cardona, and P. Vogel. *Physical Review B.* Vol. 25, p. 3878, 1982.
2. Trew, R. J., J. -B. Yan, and P. M. Mock. *Proceedings of the Institute of Electrical and Electronic Engineers.* Vol. 79, p. 598, 1991.
3. Hauver, G. E., P. H. Netherwood, R. F. Benck, and L. J. Keckes. Proceedings of the 13th Army Symposium on Solid Mechanics. Edited by S. C. Chou, F. D. Bartlett Jr., T. W. Wright, and K. Iyer, 1993.
4. Addamiano, A. *Silicon Carbide–1973.* Edited by R. C. Marshall, J. W. Faust, Jr., and C. E. Ryan, Columbia, SC: University of South Carolina, p. 179, 1974.
5. Shih, J. "Dynamic Deformation of Silicon Carbide." Ph.D. dissertation, University of California, San Diego, 1998.
6. Strossner, K., M. Cardona, and W. J. Choyke. *Solid State Communications.* Vol. 63, p. 113, 1987.
7. Aleksandrov, I. V., A. F. Goncharov, E. V. Yakovenko, and S. M. Stishov. *High-Pressure Research: Application to Earth and Planetary Sciences.* Edited by Y. Syono and M. H. Manghanani, TERRAPUB/American Geophysical Union, Tokyo, p. 409, 1992.
8. Bassett, W. A., M. S. Weathers, and T. -C. Wu. *Journal of Applied Physics.* Vol. 74, p. 3824, 1993.
9. Yoshida, M., A. Onodera, M. Ueno, K. Takemura, and O. Shimomura. *Physical Review B.* Vol. 48, p. 10587, 1993.
10. McQueen, R. G., S. P. Marsh, J. W. Taylor, J. N. Fritz, and W. J. Carter. *High Velocity Impact Phenomena.* Edited by R. Kinslow, New York: Academic Press, 1970.
11. Marsh, S. P. *LASL Shock Hugoniot Data.* Berkeley, CA: University of California, 1980.
12. Gust, W. H., A. C. Holt, and E. B. Royce. *Journal of Applied Physics.* Vol. 44, p. 550, 1973.
13. Sekine, T., and T. Kobayashi. *Physical Review B.* Vol. 55, p. 8034, 1997.
14. Sekine, T., and T. Kobayashi. *Shock Compression of Condensed Matter–1997.* Edited by S. C. Schmidt, D. P. Dandekar, and J. W. Forbes, New York: American Institute of Physics, p. 141, 1998.
15. Grady, D. E. *Journal of Applied Physics.* Vol. 75, p. 197, 1994.

16. Grady, D. E., and M. E. Kipp. Sandia Report No. SAND92-1832, Sandia National Laboratories, Albuquerque, NM, 1993.

17. Feng, R., G. F. Raiser, and Y. M. Gupta. *Journal of Applied Physics.* Vol. 79, p. 1378, 1996.

18. Bourne, N., J. Millett, and I. Pickup. *Journal of Applied Physics.* Vol. 81, p. 6019, 1997.

19. Feng, R., G. F. Raiser, and Y. M. Gupta. *Journal of Applied Physics.* Vol. 83, p. 79, 1998.

20. Yuan, G., R. Feng, and Y. M. Gupta. *Journal of Applied Physics.* Vol. 89, p. 5372, 2001.

21. Dandekar, D. P., and P. T. Bartkowski. ARL-TR-2430, U.S. Army Research Laboratory, Aberdeen Proving Ground, MD, 21001.

22. Mao, H. K., P. M. Bell, J. W. Shaner, and D. J. Steinberg. *Journal of Applied Physics.* Vol. 49, p. 3276, 1978.

23. Heinz, D. L., and R. Jeanloz. *Physical Review B.* Vol. 30, p. 6045, 1984.

24. Lambrecht, W. R., L. B. Segall, M. Methfessel, and M. van Schilfgaarde. *Physical Review B.* Vol. 44, p. 3685, 1991.

25. Hofmann, M., A. Zywietz, K. Karch, and F. Bechstedt. *Physical Review B.* Vol. 50, p. 13401, 1994.

26. Arlt, G., and G. R. Schodder. *Journal of the American Acoustical Society of America.* Vol. 37, p. 384, 1965.

27. Holmquist, T. J., A. M. Rajendran, D. W. Templeton, and K. D. Bishnoi. "A Ceramic Armor Material Database." TARDEC-TR-13754, U. S. Army Tank-Automotive Research, Development, and Engineering Center, Warren, MI, 1999.

28. Segletes, S. B. "The Vibrational Stiffness of an Atomic Lattice." ARL-TR-1757, U.S. Army Research Laboratory, Aberdeen Proving Ground, MD, 1998.

29. Birch, F. *Journal of Geophysical Research.* Vol. 83, p. 1257, 1978.

30. Jeanloz, R., and R. Grover. *Shock Compression of Condensed Matter–1988.* Edited by S. C. Schmidt and N. C. Holms, New York: Elsevier Science, p. 69, 1988.

31. Liu, J., and Y. K. Vohra. *Physical Review Letters.* Vol. 72, p. 4105, 1994.

32. Dandekar, D. P., and D. C. Benfanti. *Journal of Applied Physics.* Vol. 73, p. 673, 1993.

33. Dandekar, D. P., A. Abbate, and J. Frankel. *Journal of Applied Physics.* Vol. 76, p. 4077, 1994.

34. Asay, J. R., L. C. Chhabildas, and D. P. Dandekar. *Journal of Applied Physics.* Vol. 51, p. 4774, 1980.

35. Dandekar, D. P. *Wave Propagation and Engineering Technologies.* AMD-Vol. 188, edited by V. K. Kinra, R. J. Clifton, and G. C. Johnson. New York: ASME Press, p.131, 1994.

INTENTIONALLY LEFT BLANK.

NO. OF COPIES	ORGANIZATION
2	DEFENSE TECHNICAL INFORMATION CENTER DTIC OCA 8725 JOHN J KINGMAN RD STE 0944 FT BELVOIR VA 22060-6218
1	HQDA DAMO FDT 400 ARMY PENTAGON WASHINGTON DC 20310-0460
1	OSD OUSD(A&T)/ODDR&E(R) DR R J TREW 3800 DEFENSE PENTAGON WASHINGTON DC 20301-3800
1	COMMANDING GENERAL US ARMY MATERIEL CMD AMCRDA TF 5001 EISENHOWER AVE ALEXANDRIA VA 22333-0001
1	INST FOR ADVNCD TCHNLGY THE UNIV OF TEXAS AT AUSTIN 3925 W BRAKER LN STE 400 AUSTIN TX 78759-5316
1	US MILITARY ACADEMY MATH SCI CTR EXCELLENCE MADN MATH THAYER HALL WEST POINT NY 10996-1786
1	DIRECTOR US ARMY RESEARCH LAB AMSRL D DR D SMITH 2800 POWDER MILL RD ADELPHI MD 20783-1197
1	DIRECTOR US ARMY RESEARCH LAB AMSRL CI AI R 2800 POWDER MILL RD ADELPHI MD 20783-1197

NO. OF COPIES	ORGANIZATION
3	DIRECTOR US ARMY RESEARCH LAB AMSRL CI LL 2800 POWDER MILL RD ADELPHI MD 20783-1197
3	DIRECTOR US ARMY RESEARCH LAB AMSRL CI IS T 2800 POWDER MILL RD ADELPHI MD 20783-1197
	ABERDEEN PROVING GROUND
2	DIR USARL AMSRL CI LP (BLDG 305)

NO. OF COPIES	ORGANIZATION
1	CECOM SP & TRRSTRL COMMCTN DIV AMSEL RD ST MC M H SOICHER FT MONMOUTH NJ 07703-5203
1	PRIN DPTY FOR TCHNLGY HQ US ARMY MATCOM AMCDCGT R PRICE 5001 EISENHOWER AVE ALEXANDRIA VA 22333-0001
1	PRIN DPTY FOR ACQUSTN HQS US ARMY MATCOM AMCDCGA D ADAMS 5001 EISENHOWER AVE ALEXANDRIA VA 22333-00001
1	DPTY CG FOR RDE HQS US ARMY MATCOM AMCRD 5001 EISENHOWER AVE ALEXANDRIA VA 22333-00001
1	ASST DPTY CG FOR RDE HQS US ARMY MATCOM AMCRD COL S MANESS 5001 EISENHOWER AVE ALEXANDRIA VA 22333-00001
3	AIR FORCE ARMAMENT LAB AFATL DLJW W COOK D BELK J FOSTER EGLIN AFB FL 32542
1	DPTY ASSIST SCY FOR R & T SARD TT THE PENTAGON RM 3E479 WASHINGTON DC 20310-0103
1	DARPA L STOTTS 3701 N FAIRFAX DR ARLINGTON VA 22203-1714

NO. OF COPIES	ORGANIZATION
1	DIRECTOR US ARMY RESEARCH LAB AMSRL CS AL TA 2800 POWDER MILL ROAD ADELPHI MD 20783-1145
3	DIRECTOR US ARMY ARDEC AMSTA AR FSA E W P DUNN J PEARSON E BAKER PICATINNY ARSENAL NJ 07806-5000
2	US ARMY TARDEC AMSTRA TR R MS 263 K BISHNOI D TEMPLETON WARREN MI 48397-5000
4	COMMANDER US ARMY BELVOIR RD&E CTR STRBE N WESTLICH STRBE NAN S G BISHOP J WILLIAMS FORT BELVOIR VA 22060-5166
1	COMMANDER US ARMY RESEARCH OFFICE A RAJENDRAN PO BOX 12211 RESEARCH TRIANGLE PARK NC 27709-2211
1	NAVAL RESEARCH LAB A E WILLIAMS CODE 6684 4555 OVERLOOK AVE SW WASHINGTON DC 20375
6	DIRECTOR LANL D MANDELL P MAUDLIN R GRAY J SHANER MS F670 R DAVIDSON MS K557 F ADDESSIO G787 PO BOX 1663 LOS ALAMOS NM 87545

NO. OF COPIES	ORGANIZATION
9	DIRECTOR SANDIA NATL LABS E S HERTEL JR MS 0819 J ASAY MS 1811 R BRANNON MS 0820 L CHHABILDAS MS 1811 D CRAWFORD MS 0821 M FURNISH MS 0821 P TAYLOR ORG 1432 M KIPP MS 0820 P YARRINGTON MS 0820 PO BOX 5800 ALBUQUERQUE NM 87185-0307
10	DIRECTOR LLNL M J MURPHY J AKELLA N C HOLMES W TAO L282 J FORBES P URTIEW L282 A HOLT L290 J E REAUGH L290 W J NELLIS L299 J B CHASE L099 PO BOX 808 LIVERMORE CA 94550
3	CALTECH A INGERSOLL MS 170 25 PROF G RAVICHANDRAN T J AHRENS MS 252 21 1201 E CALIFORNIA BLVD PASADENA CA 91125
2	ARMY HIGH PERFORMANCE COMPUTING RSRCH CTR T HOLMQUIST G JOHNSON 1200 WASHINGTON AVE S MINNEAPOLIS MN 55415
2	SOUTHWEST RESEARCH INSTITUTE C ANDERSON J WALKER P O DRAWER 28510 SAN ANTONIO TX 78284

NO. OF COPIES	ORGANIZATION
2	UNIVERSITY OF DELAWARE DEPT OF MECH ENGINEERING PROF J GILLESPIE PROF J VINSON NEWARK DE 19716
3	SRI INTERNATIONAL D CURRAN D SHOCKEY R KLOPP 333 RAVENSWOOD AVE MENLO PARK CA 94025
1	VIRGINIA POLYTECHNIC INST COLLEGE OF ENGINEERING R BATRA BLACKSBURG VA 24061-0219
1	COMPUTATIONAL MECHANICS CONSULTANTS J A ZUKAS P O BOX 11314 BALTIMORE MD 21239-0314
1	KAMAN SCIENCES CORP D L JONES 2560 HUNTINGTON AVE STE 200 ALEXANDRIA VA 22303
8	INST OF ADVANCED TECH UNIVERSITY OF TX AUSTIN S BLESS H FAIR D LITTLEFIELD I MCNAB C PERSAD W REINECKE P SULLIVAN S SATAPATHY 3925 W BRAKER LN STE 400 AUSTIN TX 78759-5316
1	APPLIED RESEARCH ASSOCIATES D E GRADY 4300 SAN MATEO BLVD NE STE A220 ALBUQUERQUE NM 87110
1	INTERNATIONAL RESEARCH ASSOCIATES INC D L ORPHAL 4450 BLACK AVE PLEASANTON CA 94566

NO. OF COPIES	ORGANIZATION
1	THE DOW CHEMICAL CO CENTRAL RSRCH ENGINEERING LABORATORY M EL RAHEB BUILDING 1776 MIDLAND MI 48640
1	BOB SKAGGS CONSULTANT S R SKAGGS 79 COUNTY RD 117 SOUTH SANTA FE NM 87501
1	WASHINGTON ST UNIVERSITY SCHOOL OF MECHANCIAL AND MATERIAL ENGINEERING J L DING PULLMAN WA 99164-2920
2	WASHINGTON ST UNIVERSITY INSTITUTE OF SHOCK PHYSICS Y M GUPTA C HARI SIMHA PULLMAN WA 99164-2814
1	COORS CERAMIC COMPANY T RILEY 600 NINTH ST GOLDEN CO 80401
1	ARIZONA STATE UNIVERSITY MECHANICAL AND AEROSPACE ENGINEERING D KRAVCINOVIC TEMPE AZ 85287-6106
1	UNIVERSITY OF DAYTON RESEARCH INSTITUTE C HARI SIMHA 300 COLLEGE PARK MS SPC 1911 DAYTON OH 45469
5	DIRECTOR USARL K WILSON (5 CPS) FRENCH DEA 1396 ADELPHI MD 20783-1197

NO. OF COPIES	ORGANIZATION
	ABERDEEN PROVING GROUND
38	DIR USARL AMSRL SL BE A PRAKASH AMSRL WM E SCHMIDT T WRIGHT AMSRL WM MB G GAZONAS AMSRL WM TA P BARTKOWSKI (10) W A GOOCH T HAVEL E HORWATH H W MEYER M NORMANDIA AMSRL WM TC R COATES K KIMSEY D SCHEFFLER AMSRL WM TD J M BOTELER D DANDEKAR (10 CPS) D GROVE M RAFTENBERG E RAPACKI M SCHEIDLER T WEERASOORIYA

NO. OF COPIES	ORGANIZATION
1	DERA N J LYNCH WEAPONS SYSTEMS BUILDING A20 DRA FORT HALSTEAD SEVENOAKS KENT TN 147BP UNITED KINGDOM
2	ERNST MACH INTITUT VOLKER HOHLER H NAHAME ECKERSTRASSE 4 D 7800 FREIBURG 1 BR 791 4 GERMANY
1	FOA2 P LUNDBERG S 14725 TUMBA SWEDEN
1	PCS GROUP CAVENDISH LABORATORY W G PROUD MADINGLEY RD CAMBRIDGE UNITED KINGDOM
1	CENTRE D ETUDES DE GRAMAT J Y TRANCHET 46500 GRAMAT FRANCE
1	MINISTERE DE LA DEFENSE DR G BRAULT DGA DSP STTC 4 RUE DE LA PORTE DISSY 75015 PARIS FRANCE
1	SPART DIRECTION BP 19 DR E WARINGHAM 10 PLACE GEORGES CLEMENCEOUX 92211 SAINT CLOUD CEDEX FRANCE

NO. OF COPIES	ORGANIZATION
1	ROYAL MILITARY COLLEGE OF SCIENCE CRANEFIELD UNIVERSITY PROF N BOURNE SHRIVENHAM SWINDON SN6 8LA UNITED KINGDOM

INTENTIONALLY LEFT BLANK.

REPORT DOCUMENTATION PAGE

Form Approved
OMB No. 0704-0188

1. AGENCY USE ONLY *(Leave blank)*	2. REPORT DATE	3. REPORT TYPE AND DATES COVERED
	March 2002	Final, January–August 2001

4. TITLE AND SUBTITLE
A Survey of Compression Studies on Silicon Carbide (SiC)

5. FUNDING NUMBERS
1L162618AH80

6. AUTHOR(S)
Dattatraya P. Dandekar

7. PERFORMING ORGANIZATION NAME(S) AND ADDRESS(ES)
U.S. Army Research Laboratory
ATTN: AMSRL-WM-TD
Aberdeen Proving Ground, MD 21005-5066

8. PERFORMING ORGANIZATION REPORT NUMBER
ARL-TR-2695

9. SPONSORING/MONITORING AGENCY NAMES(S) AND ADDRESS(ES)

10.SPONSORING/MONITORING AGENCY REPORT NUMBER

11. SUPPLEMENTARY NOTES

12a. DISTRIBUTION/AVAILABILITY STATEMENT
Approved for public release; distribution is unlimited.

12b. DISTRIBUTION CODE

13. ABSTRACT *(Maximum 200 words)*

Compression of a solid material under plane shock wave propagation/ loading can provide information related to change in density and shear strength with pressure/stress of the material under inertial confinement. The present work surveys and analyzes the existing shock compression and high-pressure data on silicon carbide to provide pertinent information to material modelers and others for use in their work related to this material. It also points out a set of investigations that needs to be carried out to complement the existing data.

14. SUBJECT TERMS
equation of state, shear strength, silicon carbide

15. NUMBER OF PAGES
28

16. PRICE CODE

17. SECURITY CLASSIFICATION OF REPORT	18. SECURITY CLASSIFICATION OF THIS PAGE	19. SECURITY CLASSIFICATION OF ABSTRACT	20. LIMITATION OF ABSTRACT
UNCLASSIFIED	UNCLASSIFIED	UNCLASSIFIED	UL